Interface behaviours and mechanical properties of filling friction stir weld joining AA 2219

Y. X. Huang*[1], B. Han[1], S. X. Lv[1], J. C. Feng[1], H. J. Liu[1], J. S. Leng[2] and Y. Li[2]

In the present work, 7·8 mm thick AA 2219 rolled plates were successfully joined without keyholes using semiconsumable tools by filling friction stir welding (FFSW). The shoulder further effect was performed to enhance mechanical stir, and mechanical properties were enhanced effectively. The results showed that the bonding interface of AA 2219 bit and keyhole is defect free. The softened region on the advanced side is the weakest part of FFSW joint rather than the bonding interface of the keyhole. The average ultimate tensile strength and elongation are 172 MPa and 11·2%, equal to 90 and 82% of the base weld without defects respectively. Excellent bonding interface and mechanical properties of FFSW joints have been exhibited.

Keywords: Filling friction stir welding, Aluminium joining bit, Keyhole, Interface, Mechanical

Introduction

In the 2xxx series heat treatable aluminium alloys, AA 2219 is a binary Al–Cu alloy. The major intermetallic phase is Al_2Cu, and it has a great potential for a wide range of applications,[1–3] such as the construction of liquid cryogenic rocket fuel tanks.[4] Friction stir welding (FSW) is a relatively new solid state joining technique[5–7] as an environment friendly and energy saving processing method.[8] Friction stir welding has been widely used and acknowledged to be one of the best techniques for welding aluminium alloys. However, welding defects are formed with improper welding parameters or technological conditions.[9–11] For instance, groove, cavity and kissing bond have serious influence on joint properties.[12,13] Particularly, keyhole remains at the end of the weld inevitably, resulting from the extraction of a general non-consumable pin.[14] Obviously, the mechanical properties of joints such as lap shear, cross-tension strengths and other performances are surely limited owing to 'the weakest link effect' of the keyhole and other defects.[14,15] To repair the keyhole and defects, a lot of methods and apparatuses have been developed. Re-FSW is completely feasible to restore the defects not only outside but also inside of the joints.[16] However, another keyhole will be made again caused by the drawing of non-consumable pin.

Friction plug welding (FPW) is a solid state joining process invented by TWI. It has been applied for the space shuttle external tank in Lockheed Martin Corp. to improve the production efficiency and quality.[17] For FPW, a plug is pulled with a load after the spinning stop, which is necessary to perform a successful weld. Under the effect of strong stir and friction between the plug and the keyhole, sufficient plastic material is generated. Necessarily, excess sections of the plug need to cut.[18] The FPW has been used to repair the keyhole and other defects. However, with the use of a tapered plug without shoulder, stress concentration is formed at the interface. Nowadays, a technique called friction bit joining has been presented, in which a consumable joining bit has been applied. With the consumable joining bit, a solid state joint is formed under the cut and friction processes. Obviously, 'the weakest link effect', which is inevitably caused by the keyhole, can be solved. The consumable bit, which is made by 4140 alloy steel or D2 steel, cannot be used circularly.[19,20]

Filling friction stir welding (FFSW), adopted to repair keyholes, has been presented.[14] Using a semiconsumable tool, keyholes have been repaired based on the principle of solid state joining technique. In the present work, keyholes have been repaired by consumable AA 2219 joining bits, and the FFSW joints are further stirred by the alloy steel shoulder. Behaviours of the bonding interface between the bit and the keyhole were characterised. The mechanical properties of FFSW joints were investigated in terms of ultimate tensile strength, elongation and hardness distributions.

Experimental

The base metals were AA 2219 rolled plates with a thickness of 7·8 mm. The chemical compositions and mechanical properties are listed in Table 1. The plate was machined down to a size of 300×100 mm. The FFSW was performed using an FSW facility (FSW-3LM-003). The experiment was carried out using a tool

[1]State Key Laboratory of Advanced Welding and Joining, Harbin Institute of Technology, Harbin 150001, China
[2]Center for Composite Materials and Structures, Harbin Institute of Technology, Harbin 150001, China

*Corresponding author, email yxhuang@hit.edu.cn

Published by Maney on behalf of the Institute
Received 1 November 2011; accepted 24 December 2011
DOI 10.1179/1362171811Y.0000000100

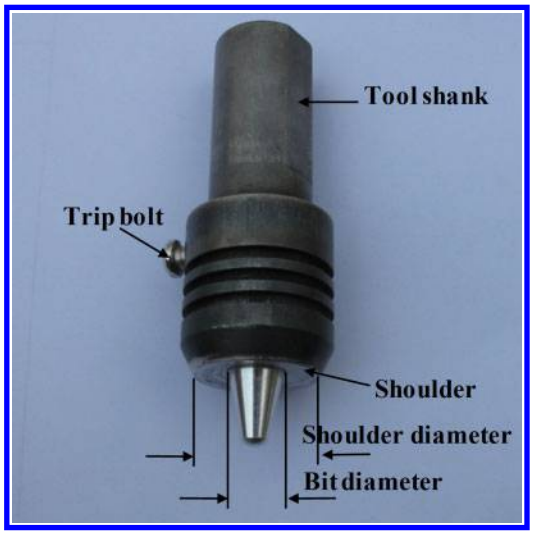

1 Photo of semiconsumable FFSW tool

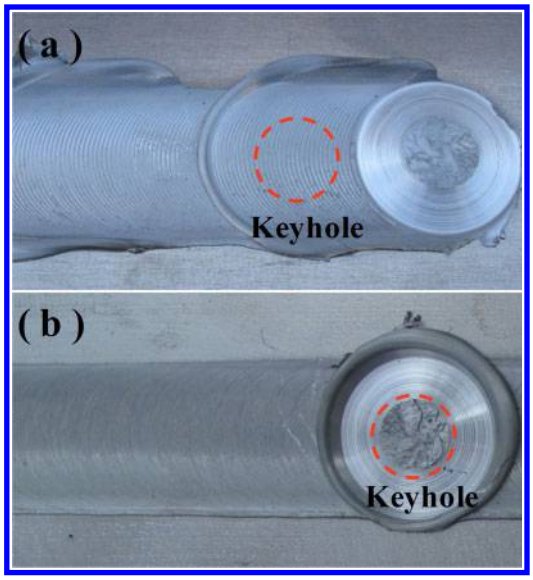

a joint with SFE; *b* joint without SFE

2 Top view of FFSW joints with different processes

with a consumable AA 2219 bit and a non-consumable alloy steel shoulder, as shown in Fig. 1. Friction stir processing (FSP), of which tool is a non-consumable alloy steel shoulder without a protruding pin, was performed to smooth and reprocess the FFSW joint. Three different tools were used to conduct FSW, FFSW and FSP respectively.[14]

For FSW, the weld parameters were selected in the range of 400–800 rev min^{-1} in rotation rate and 50–800 mm min^{-1} in traverse rate. Finally, the optimal weld parameters were found out in a limited range. They were 800 rev min^{-1} in rotation rate and 500 mm min^{-1} in traverse rate. The FFSW process for repairing was performed with a series of particular parameters, such as a rotation rate of 800 rev min^{-1}, a plunge rate of 0·5 mm min^{-1} and a deep indentation depth of 0·05 mm. With consumable AA 2219 bit plunging, materials were heated by sustaining friction. When the joining bit had been filled into the keyhole during FFSW, a following process called shoulder further effect (SFE) was used with a traverse movement of 22 mm (diameter of shoulder). The AA 2219 joining bit was cut and joined as filler material with severe plastic deformation and flow of filling metal. Sufficient mechanical friction and stir occurred. The top view of the FFSW joint with SFE in contrast with the joint without SFE is shown in Fig. 2, and the exact position of the FSW keyhole was marked with a red circle line.

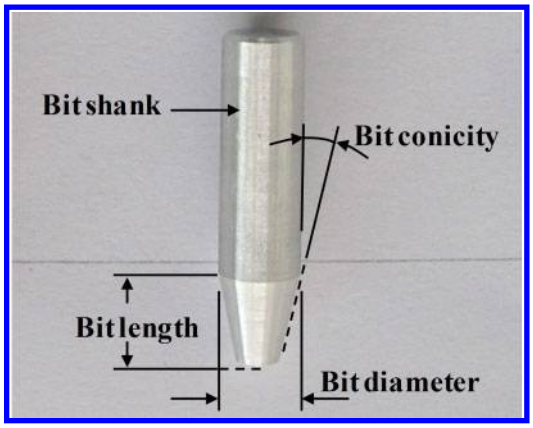

3 Photo of AA 2219 joining bit

Samples for microstructural investigation were taken from FFSW joints in lengthwise and transverse sections. The macrosection was observed by an Asana microscope (Olympus-SZX12). The microstructure of the joints' bonding interface was characterised by optical microscopy (Olympus-MPG3). Vickers microhardness measurement was performed with a load of 250 g at 10 s. Room temperature tensile test was performed at a crosshead speed of 1 mm min^{-1} by a universal testing machine (Instron-5569). The facture surface was analysed by scanning electron microscopy (Hitachi-570), and the tensile test was performed at least 96 h after FFSW, when the alloy reached a naturally aged stable condition.

Results and discussion

Process development

Six kinds of AA 2219 joining bits with different sizes were chosen for FFSW. An AA 2219 joining bit is shown in Fig. 3, of which geometric parameters were bit diameter, length and conicity. Based on the geometric parameters of keyhole, geometric parameters of bits were chosen in a range of 10–12 mm in length, 10 mm in diameter and 11–12° in conicity, as shown in Table 2. With a suitable length and conicity, the filling materials were sufficient, and a bonding interface without grooves and cavities would be achieved.

Table 1 Chemical compositions and mechanical properties of AA 2219 rolled plates

Chemical compositions/wt-%									Mechanical properties		
Al	Cu	Mn	Fe	Ti	V	Zn	Si	Zr	Tensile strength/MPa	Elongation/%	Hardness/HV
Balance	6·8	0·32	0·23	0·06	0·08	0·04	0·49	0·2	280	14·1	96

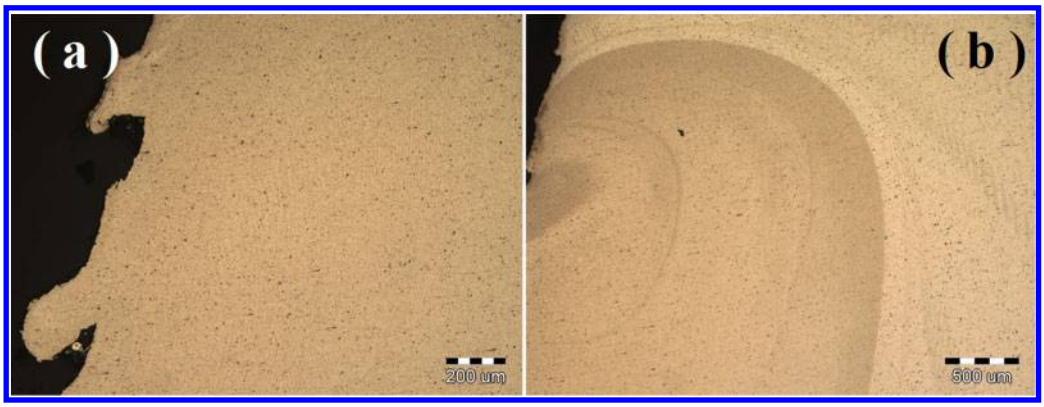

a zigzag structure; *b* onion rings

4 Details of keyhole

During FFSW process, the lengthening bit was certainly positive to heat generation. The length of the joining bit was significant in avoiding defects. In addition, SFE is an effective and important process. The filling material is mixed adequately by shoulder stir. The interface microstructures showed that defects, especially cavities, were formed at the bottom with unreasonably short lengths. Bit conicity was also quite important and significant. If the bit was too big and mismatched to plunge into the keyhole, defects were formed along the bonding interface of the bit and keyhole, especially at bottom of the keyhole. Furthermore, the joint was destructive as surplus material extrusion. The optimal parameters of FSW, FFSW, SFE and FSP are summarised in Table 3. These welding parameters were determined based on a series of preparatory experiments for optimisation, in which several parameters were tried including rotation rates and traverse speeds. For FFSW without SFE, the FFSW tool lifted directly as soon as the bit had been filled into the keyhole. The interface between the bit and the keyhole was clear, and materials were not mixed sufficiently. By SFE, large grains near the surface of the joint broke. Filling materials were mixed adequately, and the interface in quasi-nugget zone disappeared. Intercavities, flaws and weak interface were closed and merged. The FFSW joint was strengthened.

Table 2 Geometric parameters of AA 2219 joining bits

Sample no.	Bit diameter/mm	Bit length/mm	Bit conicity/°
1	10	10	11
2	10	10	12
3	10	11	11
4	10	11	12
5	10	12	11
6	10	12	12

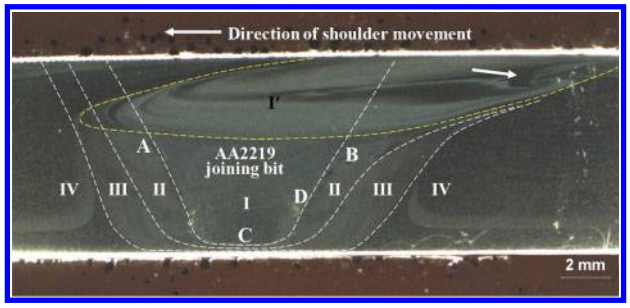

5 Lengthwise section of typical FFSW joint of 7·8 mm AA 2219 plates composed of five distinct zones

Macro- and microstructures of FFSW joints

Details of the keyhole are shown in Fig. 4. The zigzag structure was obvious along the border, which was formed from the extraction of non-consumable pin (*see* Fig. 4*a*). In addition, onion rings were observed with cyclical thermomechanical effects during FSW (*see* Fig. 4*b*). Figure 5 shows a macrosection of a typical FFSW joint, which was taken from the lengthways plane. As a result of the combined operations of FFSW and FSP, the joint consisted of five distinct zones (*see* labels in Fig. 5), which are called filled zone, quasi-nugget zone, thermomechanically affected zone, heat affected zone and nugget zone respectively.[14] In FFSW, heat was generated due to both friction and plastic deformation at the interface. The filled zone was mainly composed of AA 2219 joining bit. The thermomechanically affected zone experienced both elevated temperature and plastic deformation. By SFE, the shape of the nugget zone was changed and asymmetric. The size of the nugget zone was larger than that of the nugget zone without SFE. Stirring and mixing of near surface material were more sufficient. Furthermore, the nugget zone extended to the backside of the shoulder, which was opposite to the direction of traverse, as shown by the arrowhead in Fig. 5. Friction and stir were enhanced

Table 3 Optimised welding parameters for FSW, FFSW, SFE and FSP

Process	Rotation rate/rev min^{-1}	Traverse speed/mm min^{-1}	Plunge speed/mm min^{-1}	Deep indentation depth/mm	Tilt angle/°
FSW	800	500	3·0	0·2	2·5
FFSW	800	…	0·5	0·1	2·5
SFE	800	500	…	0·1	2·5
FSP	800	500	0·5	0·1	2·5

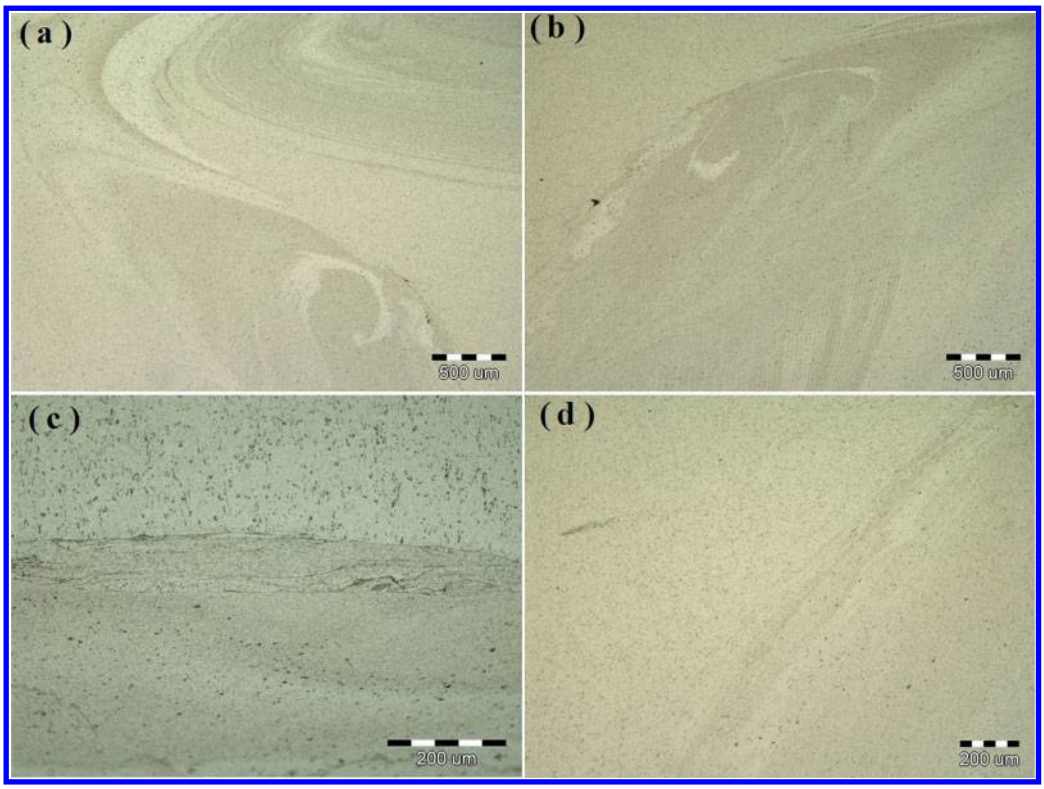

a-d refer to the four locations labelled in Figure 5

6 Interface details of FFSW joint

with the increase in deep indentation depth, and the area of nugget zone increased.

Figure 6 presented the details of the bonding interface at four typical locations (*see* labels in Fig. 5). Solid state bonding between the aluminium bit and the keyhole was achieved. The welded joint was fundamentally defect free, and the zigzag structure in Fig. 4 totally disappeared and was replaced by a perfect bonding interface.

Tensile properties of FFSW joints

In Fig. 7, the top view and macroimage of a filled FFSW joint sectioned in the transverse plane are described. As shown in Fig. 7*a*, the fracture position of an unfilled joint was located at the point of the keyhole, and the keyhole was the weakest part for the FSW joint. As shown in Fig. 7*b* and *c*, the fracture of the FFSW joint was located at the border of the thermomechanically affected zone and heat affected zone on the advanced side. The angle between the fracture and the horizontal line was ~45°, and the fracture indicated a failed type of ductile fracture.

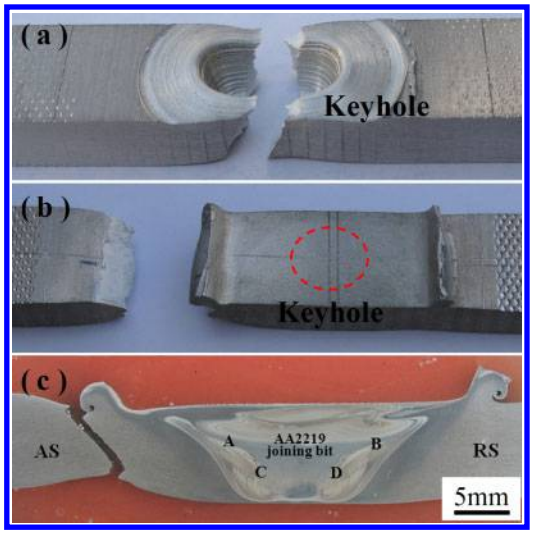

a view of failed keyhole; *b* view of failed FFSW joint; *c* cross-section of failed FFSW joint

7 View of failed FSW and FFSW joints

Figure 8 presents the microscopic appearances of the bonding interface between the joining bit and the keyhole at four different locations (*see* labels in Fig. 7*b*) after tensile test. For microimage, the bonding interface was kept intact without any obvious flaws, and it was similar to the original interface in Fig. 6. Excellent tensile properties of FFSW joints were performed. The bonding interface was no longer the weakest part. Transverse tensile properties of FFSW joints are shown in Fig. 9, of which the geometric parameters of the joining bits are listed in Table 2. All these FFSW joints were welded with optimised parameters listed in Table 3. As shown in Fig. 9, the tensile properties of FFSW joints were relatively stable with the change in size of AA 2219 joining bits. The maximum ultimate tensile strength is 174·7 MPa, nearly 95% of the FSW weld strength. The maximum elongation is 14·2%, equal to the FSW weld elongation. The average value of ultimate strength was ~172 MPa, equal to 90% of the FSW weld strength, and the average value of elongations was 11·2%, nearly 82% of the base weld. For the FSW joint, the average values of ultimate tensile strength and elongation were ~65·6 and 97·2% of the base material respectively. Figure 10 displays the tensile fractured morphologies of a typical FFSW joint. The fractured surface was characterised by dimples and tearing edges, and plastic deformation occurred. Obviously, the FSW keyholes were repaired successfully by FFSW with SFE.

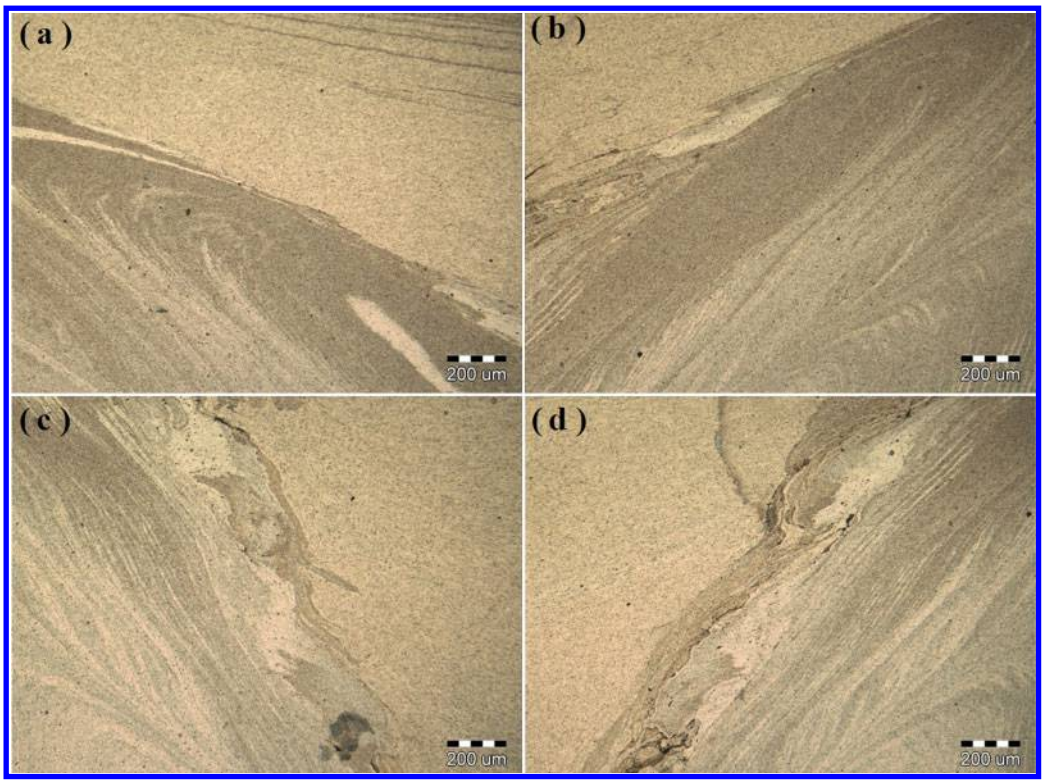

a-d refer to the four locations labelled in Figure 7c

8 Interface details of failed FFSW joint

Hardness distribution of FFSW joint

The tensile properties and fracture locations of the joints were dependent on the microhardness distributions and the weld defects of the joints.[21] When the welding speed was slower than a certain critical value, the tensile properties and fracture locations of defect free joints were dependent on microhardness distribution.[22] The microhardness distribution of the FFSW joint sectioned in the transverse plane is shown in Fig. 11. The hardness of the base material was in the range of 90–100 HV. The hardness gradually decreased to the lowest value and showed a dramatic increase towards the weld centre. The hardness profile exhibited a 'W-type' symmetry. In measuring range, the hardness in the filled zone revealed the highest value of 80 HV. The hardness between the thermomechanically affected zone and heat affected zone showed the lowest value of 45 HV on both sides. This was attributed to the weakening of precipitate deterioration and solid solution. Fracture location was closely related with the microhardness distribution of FFSW joint. Fracture location was on the advanced side.

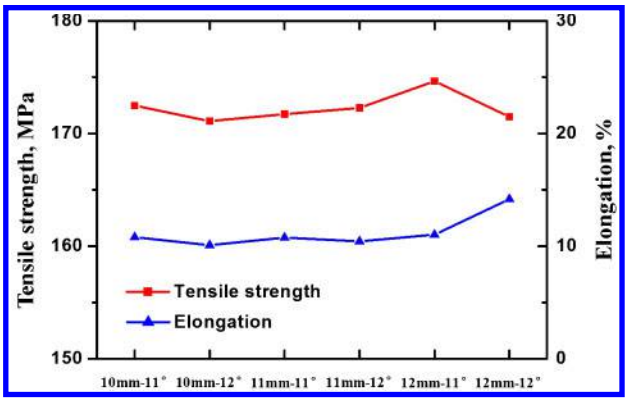

9 Tensile strengths and elongations of FFSW joints

The FFSW belongs to a kind of solid state welding technique. Materials that are difficult to be joined by conventional fusion welding techniques will be defect free when joined by FFSW. Aluminium alloys with different heat treatment conditions, which can be welded by FSW ideally, also can be welded by FFSW. The keyhole of FSW seam can be repaired by FFSW. Combined with re-FSW, FFSW can also repair other defects. First, re-FSW can be used to repair defects, such as groove, cavity and kissing bond. Second, FFSW is applied to repair the keyhole left by the re-FSW process. Combined with FFSW, FSW without a keyhole can be realised. In the subsequent study, different bit materials will be tried such as AA 7075, and the effect of increasing bit plunge rate will be studied particularly.

Conclusions

Filling friction stir welding has been proposed to successfully repair the keyhole using a semiconsumable tool consisting of an alloy steel shoulder and an AA 2219 joining bit. The shoulder of the semiconsumable tool can be used circularly. The SFE process enhances the mechanical properties of FFSW joint effectively. The area of the nugget zone is increased, and the shape is changed and is asymmetric. The bonding interface is kept intact without any flaws after tensile test. The softening region between the thermomechanically affected zone and heat affected zone on the advanced side is the weakest part rather than the refilled keyhole. For FFSW joints, the average values of ultimate tensile strength and elongation are 172 MPa and 11·2%, equal to 90 and 82% of the base FSW weld respectively. Superior defect free interface and excellent

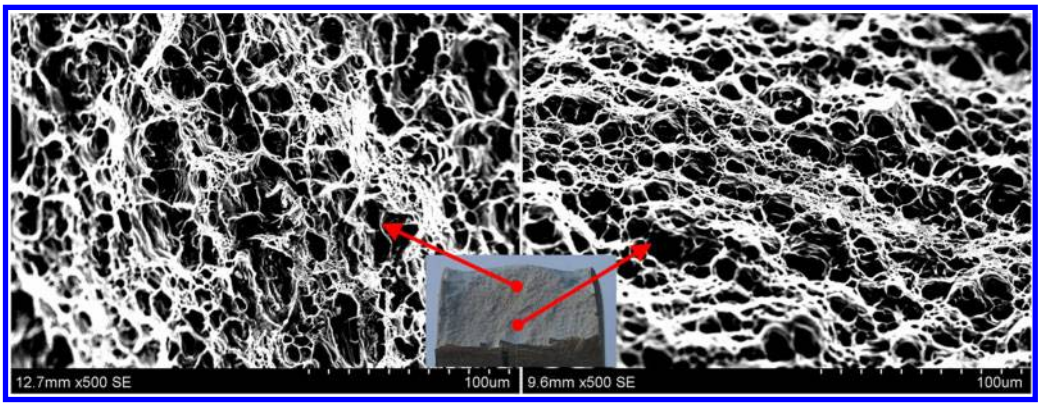

10 Microimage of FFSW joint tensile fractured appearance

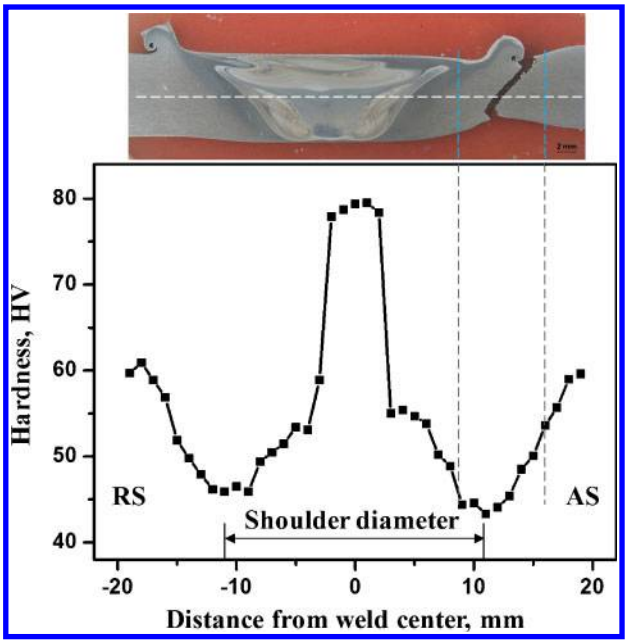

11 Vickers microhardness distribution measured across midline

mechanical properties of FFSW joints have been exhibited obviously.

Acknowledgements

The work was jointly supported by the National Natural Science Foundation of China (grant no. 50904020), the Science and Technology Innovation Research Project of Harbin for Young Scholar (grant no. 2009RFQXG050), the Fundamental Research Funds for the Central Universities (grant no. HIT.NSRIF.2012007) and the China Postdoctoral Science Foundation (grant nos. 20090460883 and 201003419).

References

1. C. Huang and S. Kou: 'Partially melted zone in aluminum welds – liquation mechanism and directional solidification', *Weld. J.*, 2000, **79**, 113–120.
2. A. C. Nunes, E. O. Bayless, C. S. Jones, P. M. Munafo, A. P. Biddle and W. A. Wilson: 'Variable polarity plasma arc welding on the space shuttle external tank', *Weld. J.*, 1984, **63**, (9), 27–35.
3. G. Albertini, G. Bruno, B. D. Dunn, F. Fiori, W. Reimers and J. S. Wright: 'Comparative neutron and X-ray residual stress measurements on Al-2219 welded plate', *Mater. Sci. Eng. A*, 1997, **A224**, 157–165.
4. W. F. Xu, J. H. Liu, G. H. Luan and C. L. Dong: 'Microstructure and mechanical properties of friction stir welded joints in 2219-T6 aluminum alloy', *Mater. Des.*, 2009, **30**, 3460–3467.
5. W. M. Thomas, E. D. Nicholas, J. C. Needham, M. G. Murch, P. Temple-Smith and C. J. Dawes: Friction stir welding. International Patent PCT/GB92/02203 and GB Patent 9125978·9, 1991.
6. W. M. Thomas and E. D. Nicholas: 'Friction stir welding for the transportation industries', *Mater. Des.*, 1997, **18**, 269–273.
7. R. S. Mishra and Z. Y. Ma: 'Friction stir welding and processing', *Mater. Sci. Eng. R*, 2005, **R50**, 1–78.
8. B. Li, Y. F. Shen and W. Y. Hu: 'The study on defects in aluminum 2219-T6 thick butt friction stir welds with the application of multiple non-destructive testing methods', *Mater. Des.*, 2011, **32**, 2073–2084.
9. H. J. Liu, Y. C. Chen and J. C. Feng: 'Effect of zigzag line on the mechanical properties of friction stir welded joints of an Al–Cu alloy', *Scr. Mater.*, 2006, **55**, 231–234.
10. H. Zhang, S. B. Lin, L. Wu, J. C. Feng and S. L. Ma: 'Defects formation procedure and mathematic model for defect free friction stir welding of magnesium alloy', *Mater. Des.*, 2006, **27**, 805–809.
11. Y. G. Kim, H. Fujii, T. Tsumura, T. Komazaki and K. Nakata: 'Three defect types in friction stir welding of aluminum die casting alloy', *Mater. Sci. Eng. A*, 2006, **A415**, 250–254.
12. T. L. Dickerson and J. Przydatek: 'Fatigue of friction stir welds in aluminium alloys that contain root flaws', *Int. J. Fatigue*, 2003, **25**, 1399–1409.
13. M. N. James, G. R. Bradley, D. G. Hattingh, D. J. Hughes and P. J. Webster: 'Residual stresses, defects and fatigue cycling in friction stir butt welds in 5383-H321 and 5083-H321 aluminum alloys', *Mater. Sci. Forum*, 2003, **426**, 2915–2920.
14. Y. X. Huang, B. Han, Y. Tian, H. J. Liu, S. X. Lv, J. C. Feng, J. S. Leng and Y. Li: 'New technique of filling friction stir welding', *Sci. Technol. Weld. Join.*, 2011, **16**, 497–501.
15. T. Huang, Y. S. Sato, H. Kokawa, M. P. Miles, K. Kohkonen, B. Siemssen, R. J. Steel and S. Packer: 'Microstructural evolution of DP980 steel during friction bit joining', *Mater. Sci. Eng. A*, 2009, **A40**, 2994–3000.
16. H. J. Liu and H. J. Zhang: 'Repair welding process of friction stir welding groove defect', *Trans. Nonferrous Met. Soc. China*, 2009, **19**, 563–567.
17. P. J. Hartley: 'Friction plug weld repair for the space shuttle external tank', *Weld. Met. Fab.*, 2002, **9**, 6–8.
18. T. Riki, T. L. Hibbard and L. A. Kenner: 'Friction plug welding', US Patent 141294, 1998.
19. M. P. Miles, Z. Feng, K. Kohkonen, B. Weickum, R. Steel and L. Lev: 'Spot joining of AA 5754 and high strength steel sheets by consumable bit', *Sci. Technol. Weld. Join.*, 2010, **15**, 325–330.
20. M. P. Miles, K. Kohkonen, S. Packer, R. Steel, B. Siemssen and Y. S. Sato: 'Solid state spot joining of sheet materials using consumable bit', *Sci. Technol. Weld. Join.*, 2009, **14**, 72–77.
21. H. J. Liu, H. Fujii, M. Maeda and K. Nogi: Proc. 3rd Int. Symp. on 'Friction stir welding', Kobe, Japan, September 2001, TWI Ltd. S5-P2.
22. Y. C. Chen, H. J. Liu and J. C. Feng: 'Friction stir welding characteristics of different heat-treated-state 2219 aluminum alloy plates', *Mater. Sci. Eng. A*, 2006, **A420**, 21–25.